

Analysis of the entanglement between two individual atoms using global Raman rotations

A. Gaëtan, C. Evellin, J. Wolters, P. Grangier, T. Wilk and A. Browaeys

*Laboratoire Charles Fabry, Institut d'Optique,
CNRS, Univ Paris-Sud, Campus Polytechnique,
RD 128, 91127 Palaiseau cedex, France*

(Dated: September 24, 2018)

Abstract

Making use of the Rydberg blockade, we generate entanglement between two atoms individually trapped in two optical tweezers. In this paper we detail the analysis of the data and show that we can determine the amount of entanglement between the atoms in the presence of atom losses during the entangling sequence. Our model takes into account states outside the qubit basis and allows us to perform a partial reconstruction of the density matrix describing the two atom state. With this method we extract the amount of entanglement between pairs of atoms still trapped after the entangling sequence and measure the fidelity with respect to the expected Bell state. We find a fidelity $F_{\text{pairs}} = 0.74(7)$ for the 62% of atom pairs remaining in the traps at the end of the entangling sequence.

PACS numbers: 32.80.Rm, 03.67.Bg, 32.80.Pj, 42.50.Ct, 42.50.Dv

INTRODUCTION

Entanglement between two particles can be generated by designing and manipulating interactions between them. For example, the entanglement in ion systems relies on the Coulomb interaction between the ions [1]. Entanglement is therefore difficult to produce in neutral atom systems, due to their weaker interactions. One solution, implemented in the first demonstration of entanglement between neutral atoms, makes use of a high-Q cavity to mediate the interaction between transient atoms [2]. Another more recent approach uses ultra-cold atoms in optical lattices and the short-range s-wave interaction that occurs when their wavepackets overlap. This leads to the preparation of entangled states of a chain of atoms [3] or pairs of atoms [4]. This approach requires ground state cooling of atoms in their trapping potential and the ability to overlap their wavepackets during a controllable amount of time. Furthermore, although there has been tremendous progress in this direction recently [5], it is not easy to address atoms in optical lattices with a spacing between the wells of less than a micrometer. An alternative approach is to store atoms in traps that are separated by several micrometers in order to have addressability using standard optical techniques, and to avoid motional control of the atoms [6, 7]. One then needs an interaction which can act at long distance. Atoms in Rydberg states do provide such a long range interaction, which can reach several MHz at a distance of 10 micrometers. Moreover, this interaction can be switched on and off at will by placing the atoms in a Rydberg state for a controllable amount of time. This approach using Rydberg interaction has been proposed theoretically as a way to perform fast quantum gates [8, 9, 10] and is intrinsically deterministic and scalable to more than two atoms. Recent proposals extend this idea to the generation of various entangled states [11, 12].

Recently, two experiments implemented Rydberg interactions to demonstrate a cNOT gate [13] and to generate entanglement between two atoms trapped in optical tweezers [14]. In the present paper, we analyze in detail the experiment of reference [14]. We explain how we extract the amount of entanglement with a method based on global rotations of the state of the atoms.

The paper is organized as follows. In section we present the principle of the experiment. In section we detail the setup as well as the experimental sequence. We show that some atoms are lost during the sequence. In section we present the model used to extract the

amount of entanglement, which takes into account the loss of atoms. In the following sections we present the experimental results: in section we quantify the atom losses and in section we describe the partial tomography of the density matrix, extract the value of the fidelity and discuss the factors limiting this value.

RYDBERG BLOCKADE AND ENTANGLEMENT

The principle of the experiment relies on the Rydberg blockade effect demonstrated recently with two single atoms [15, 16]. Due to their large electric dipole when they are in a Rydberg state $|r\rangle$, two atoms a and b interact strongly if they are close enough. This interaction leads to a shift ΔE of the doubly excited state $|r, r\rangle$.

As a consequence, a laser field coupling a ground state $|\uparrow\rangle$ and a Rydberg state $|r\rangle$ (with Rabi frequency $\Omega_{\uparrow r}$) cannot excite both atoms at the same time, provided that the linewidth of the excitation is smaller than ΔE . In this blockade regime, the two-atom system behaves like an effective two-level system [16]: the ground state $|\uparrow, \uparrow\rangle$ is coupled to the excited state

$$|\Psi_r\rangle = \frac{1}{\sqrt{2}}(e^{i\mathbf{k}\cdot\mathbf{r}_a}|r, \uparrow\rangle + e^{i\mathbf{k}\cdot\mathbf{r}_b}|\uparrow, r\rangle), \quad (1)$$

where $\mathbf{k} = \mathbf{k}_R + \mathbf{k}_B$ is the sum of the wave vectors of the red (R) and blue (B) lasers used for the two-photon excitation (see section and figure 1b) and $\mathbf{r}_{a/b}$ are the positions of the atoms. The coupling strength between these states is enhanced by a factor $\sqrt{2}$ with respect to the one between $|\uparrow\rangle$ and $|r\rangle$ for a single atom [16]. Thus, starting from $|\uparrow, \uparrow\rangle$, a pulse of duration $\pi/(\sqrt{2}\Omega_{\uparrow r})$ prepares the state $|\Psi_r\rangle$. To produce entanglement between the atoms in two ground states, the Rydberg state $|r\rangle$ is mapped onto another ground state $|\downarrow\rangle$ using the same blue laser and an additional red laser (wave vector \mathbf{k}'_R) with a pulse of duration $\pi/\Omega_{r\downarrow}$ ($\Omega_{r\downarrow}$ is the two-photon Rabi frequency). This sequence results in the entangled state

$$|\Psi\rangle = \frac{1}{\sqrt{2}}(|\downarrow, \uparrow\rangle + e^{i\phi}|\uparrow, \downarrow\rangle), \quad (2)$$

with $\phi = (\mathbf{k}_R - \mathbf{k}'_R) \cdot (\mathbf{r}_b - \mathbf{r}_a)$, assuming that the positions of the atoms are frozen [25]. As the light fields are propagating in the same direction and the energy difference between the two ground states is small, $\mathbf{k}_R \simeq \mathbf{k}'_R$. This procedure therefore generates in a deterministic way the well defined entangled state with $\phi = 0$, which is the $|\Psi^+\rangle$ Bell state.

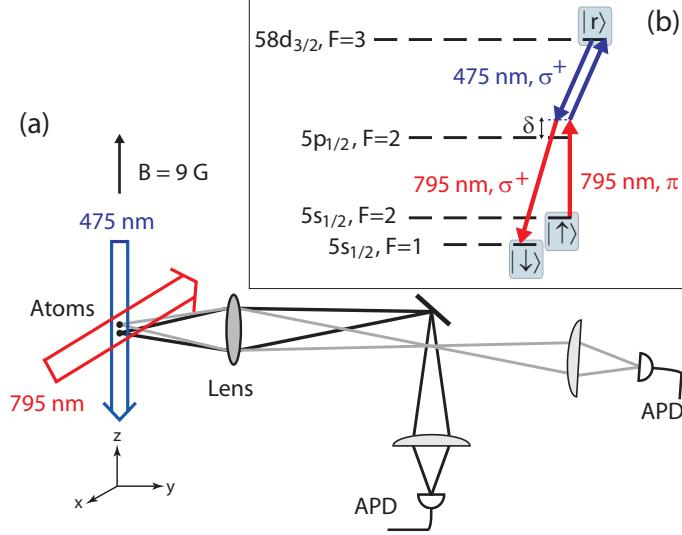


FIG. 1: (a) Experimental setup. Two atoms are held at a distance of $4 \mu\text{m}$ in two optical tweezers formed by focused laser beams at 810 nm (not shown). The fluorescence of each atom is directed onto separate avalanche photodiodes (APDs). The σ^+ -polarized 475 nm laser has a waist of $25 \mu\text{m}$ and is directed along the z -axis, the two 795 nm lasers have waists of $130 \mu\text{m}$, copropagate along the x -axis and have both linear polarization, one along the quantization axis, the other perpendicular. The 475 nm and 795 nm lasers have powers of 30 mW and 15 mW, respectively, which correspond to Rabi frequencies $\Omega_B/(2\pi) \sim 25$ MHz and $\Omega_R/(2\pi) \sim 300$ MHz. (b) Atomic level structure and lasers used for the excitation towards the Rydberg state. The 475 nm laser and the two 795 nm lasers are tuned to the two photon transitions from $|\uparrow\rangle$ to $|r\rangle$ and from $|r\rangle$ to $|\downarrow\rangle$.

EXPERIMENTAL SETUP AND PROCEDURE

Our experimental setup is depicted in Fig. 1(a). Two ^{87}Rb atoms are held in two optical tweezers separated by $4 \mu\text{m}$. The interatomic axis is aligned with a magnetic field ($B=9$ G), which defines the quantization axis and lifts the degeneracy of the Zeeman sublevels. The tweezers are formed by two laser beams at 810 nm which are sent at a small angle through a microscope objective focusing the beams to a waist of $0.9 \mu\text{m}$. Atoms are captured from an optical molasses and, due to the small trapping volume, either one or no atom is captured in each trap [17]. The same objective collects the fluorescence light of the atoms induced by the molasses beams at 780 nm. The light coming from each trapped atom is directed onto separate avalanche photodiodes (APDs) which allows us to discriminate for each trap

whether an atom is present or not.

The relevant levels of ^{87}Rb are shown in Fig. 1(b). We have chosen the Rydberg state $|r\rangle = |58d_{3/2}, F = 3, M = 3\rangle$. The interaction energy between two atoms in this state is enhanced by a Förster resonance [18] which leads to a calculated interaction energy $\Delta E/h \approx 50$ MHz for a distance between the atoms of $4 \mu\text{m}$ [16]. The qubit ground states considered for the entanglement are $|\downarrow\rangle = |F = 1, M = 1\rangle$ and $|\uparrow\rangle = |F = 2, M = 2\rangle$ of the $5s_{1/2}$ manifold, separated in frequency by 6.8 GHz. To excite one atom from $|\uparrow\rangle$ to $|r\rangle$, we use a two-photon transition with a π -polarized laser at 795 nm and a σ^+ -polarized laser at 475 nm. The frequency of the 795 nm laser is blue-detuned by $\delta=600$ MHz from the transition from $|\uparrow\rangle$ to $(5p_{1/2}, F = 2)$ in order to reduce spontaneous emission. The measured Rabi frequency of the two-photon transition from $|\uparrow\rangle$ to $|r\rangle$ is $\Omega_{\uparrow r}/2\pi \approx 6$ MHz for a single atom. We use the same 475 nm laser for the transition from $|r\rangle$ to $|\downarrow\rangle$, but a second 795 nm laser, linearly polarized perpendicular to the quantization axis, with a frequency 6.8 GHz higher to address state $|\downarrow\rangle$. The measured Rabi frequency for this second two-photon transition is $\Omega_{r\downarrow}/2\pi \approx 5$ MHz. The two 795 nm lasers are phase-locked to each other using a beat-note technique and fast electronic correction. The two lasers are also used to drive Raman rotations between the qubit states $|\uparrow\rangle$ and $|\downarrow\rangle$. We observe Rabi oscillations between $|\uparrow\rangle$ and $|\downarrow\rangle$ with an amplitude of 0.95, which includes the fidelity of state initialization and state detection. We set the Rabi frequency of the Raman transition to $\Omega_{\uparrow\downarrow} = 2\pi \times 250$ kHz.

We read out the atomic state by applying a push-out laser beam resonant to the $F=2$ to $F=3$ transition of the D2-line [19], which ejects atoms that are in state $|\uparrow\rangle$ (or in other M -states of the $F = 2$ ground level) from the trap. Only atoms that are in $|\downarrow\rangle$ (or in other M -states of the $F = 1$ level) will stay in the trap and will be detected.

The experimental sequence is shown in figure 2. An experiment starts upon detection of an atom in each trap (trap depth 3.5 mK). After turning off the cooling beams, we ramp adiabatically the trap depth down to 0.5 mK and optically pump the atoms in $|\uparrow\rangle$ [26]. This is done by a $600 \mu\text{s}$ optical pumping phase with a σ^+ -polarized laser coupling the levels $(5s_{1/2}, F = 2)$ and $(5p_{3/2}, F = 2)$ and a repumping laser from $(5s_{1/2}, F = 1)$ to $(5p_{3/2}, F = 2)$. Afterwards we switch off the dipole trap while we apply the excitation and mapping pulses towards the Rydberg state and back. The excitation pulse has a duration of $\pi/(\sqrt{2}\Omega_{\uparrow r}) \approx 70$ ns to excite state $|\Psi_r\rangle$. The mapping pulse has a duration $\pi/\Omega_{r\downarrow} \approx 110$ ns. The trap is then turned on again. In order to analyze the produced two-atom state, we drive

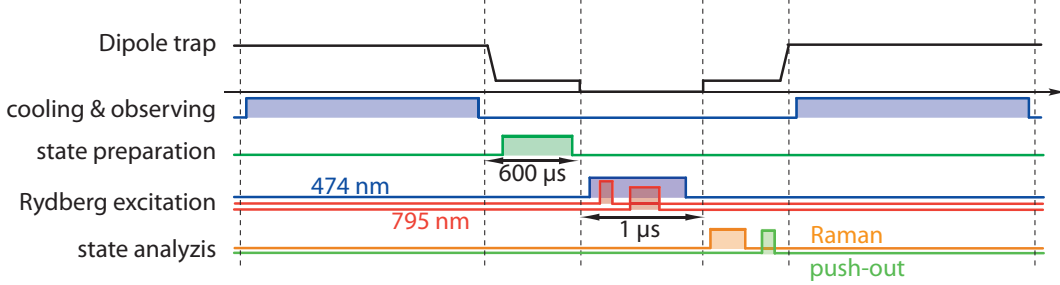


FIG. 2: Experimental sequence used to entangle two atoms and analyze the entanglement. The state preparation is done by optical pumping. For clarity the horizontal time axis is not on scale.

global Raman rotations on the two atoms (see below) and the push-out laser is applied. Subsequently, we ramp up the depth of the dipole trap to its initial value and record for each trap whether the atom is present or not. We repeat the experiment 100 times for each Raman rotation angle $\theta = \Omega_{\uparrow\downarrow}\tau$ (τ is the duration of the Raman pulse). We then extract the probabilities $P_a(\theta)$ and $P_b(\theta)$ to recapture an atom in trap a or b , the joint probabilities $P_{01}(\theta)$ and $P_{10}(\theta)$ to lose atom a and recapture atom b or vice versa, as well as probabilities $P_{11}(\theta)$ and $P_{00}(\theta)$ to recapture or lose both atoms, respectively, assigning 0 to a loss and 1 to a recapture.

Our state-detection scheme, based on the push out technique, identifies any atom a or b when it is in state $|\downarrow\rangle$ [27]. However, it does not discriminate between atoms in state $|\uparrow\rangle$ and atoms that could be lost during the sequence. As a consequence we have to evaluate the amount of these additional losses. We have measured in a separate experiment the probability p_{recap} to recapture a pair of atoms after the excitation and mapping pulses, without applying the push-out laser. We have found $p_{\text{recap}} = 0.62(3)$, which shows that the losses of one or both atoms cannot be neglected. We have incorporated these losses in the analysis of our measurement results, using a model that is detailed in the next section.

THEORETICAL MODEL

To take into account the loss of atoms, we introduce a set of additional states $\{|x\rangle\}$, extending the basis of each atom to $(|\uparrow\rangle, |\downarrow\rangle, \{|x\rangle\})$ and we describe the two-atom system by the density matrix $\hat{\rho}$ in this extended basis. We assume that these additional states $\{|x\rangle\}$, corresponding to an atom leaving the qubit basis, cannot be distinguished from state

$|\uparrow\rangle$ by the state detection. The exact nature of states $\{|x\rangle\}$ will be detailed in section , but we already note that in our case they can come either from an atom leaving its trap (physical loss) or from an atom still trapped but ending up in an unwanted state, outside the qubit basis $\{|\uparrow\rangle, |\downarrow\rangle\}$. The losses of one or two atoms are given by the sum of the diagonal elements $L_{\text{total}} = \sum_x (P_{\uparrow x} + P_{\downarrow x} + P_{x\uparrow} + P_{x\downarrow}) + \sum_{x,x'} P_{xx'}$.

We assume that the states $\{|x\rangle\}$ are not coupled to $|\downarrow\rangle$ or $|\uparrow\rangle$ by the Raman lasers, and that they are not coupled between each other. The Raman rotation for the two atoms can then be described by the operator $R_{a\otimes b}(\theta, \varphi) = R_a(\theta, \varphi) \otimes R_b(\theta, \varphi)$ where $R_{a/b}(\theta, \varphi)$ is given by the matrix

$$R_{a/b}(\theta, \varphi) = \begin{pmatrix} \cos \frac{\theta}{2} & ie^{i\varphi} \sin \frac{\theta}{2} & 0 \\ ie^{-i\varphi} \sin \frac{\theta}{2} & \cos \frac{\theta}{2} & 0 \\ 0 & 0 & \hat{1} \end{pmatrix}_{|\uparrow\rangle, |\downarrow\rangle, \{|x\rangle\}}, \quad (3)$$

where $\hat{1}$ stands for the identity matrix, $\theta = \Omega_{\uparrow\downarrow}\tau$ and φ is the phase difference between the two Raman lasers. The two atoms are exposed to the same laser field and undergo a rotation with the same θ and φ . After the rotation the density matrix of the produced state is $\hat{\rho}_{\text{rot}}(\theta, \varphi) = R_{a\otimes b}(\theta, \varphi)\hat{\rho}_{a\otimes b}^\dagger(\theta, \varphi)$. The idea behind this approach is to transform the coherences (off-diagonal matrix element) into populations that can be directly measured.

In our experiment, we do not control the phase φ of the Raman lasers with respect to the phase of the atomic states. This comes ultimately from the fact that the atoms are loaded in the dipole traps at random, so that there is no phase relation with respect to the microwave used to generate the Raman transition. This phase φ varies randomly from shot-to-shot over 2π . Our measurement results are therefore averaged over φ . When averaging $\langle \hat{\rho}_{\text{rot}}(\theta, \varphi) \rangle_\varphi$, all coherences of $\hat{\rho}_{\text{rot}}$ average out, apart from the off-diagonal element $\rho_{\downarrow\uparrow, \uparrow\downarrow}$ relevant to characterize state $|\Psi^+\rangle$. We then calculate the expressions averaged over φ of the probabilities $P_{a/b}(\theta)$ as well as $P_{11}(\theta)$ and $\Pi(\theta) = P_{11}(\theta) + P_{00}(\theta) - P_{01}(\theta) - P_{10}(\theta)$ as a function of the matrix elements of $\hat{\rho}$.

As our state detection identifies a recapture (1) with the atom being in state $|\downarrow\rangle$, we get

for the probability to recapture atom a independently of the state of atom b :

$$\begin{aligned}
P_a(\theta) &= P_{\downarrow\downarrow}(\theta) + P_{\uparrow\uparrow}(\theta) + \sum_x P_{\downarrow x}(\theta) \\
&= \frac{1}{2} \left[P_{\uparrow\downarrow} + P_{\downarrow\uparrow} + P_{\uparrow\uparrow} + P_{\downarrow\downarrow} + \sum_x (P_{x\uparrow} + P_{x\downarrow}) \right] \\
&\quad + \frac{1}{2} \left[P_{\downarrow\downarrow} - P_{\uparrow\uparrow} + P_{\downarrow\uparrow} - P_{\uparrow\downarrow} + \sum_x (P_{x\downarrow} - P_{x\uparrow}) \right] \cos \theta .
\end{aligned} \tag{4}$$

In this formula and in the following ones, $P_{n,m}(\theta) = \langle n, m | \hat{\rho}_{\text{rot}} | n, m \rangle$, and $P_{n,m} = P_{n,m}(0)$ with $\{n, m\} \in \{\downarrow, \uparrow, x\}$. Similarly, the probability to recapture atom b independently of the state of atom a is

$$\begin{aligned}
P_b(\theta) &= P_{\downarrow\downarrow}(\theta) + P_{\uparrow\uparrow}(\theta) + \sum_x P_{x\downarrow}(\theta) \\
&= \frac{1}{2} \left[P_{\uparrow\downarrow} + P_{\downarrow\uparrow} + P_{\uparrow\uparrow} + P_{\downarrow\downarrow} + \sum_x (P_{x\uparrow} + P_{x\downarrow}) \right] \\
&\quad + \frac{1}{2} \left[P_{\downarrow\downarrow} - P_{\uparrow\uparrow} + P_{\uparrow\downarrow} - P_{\downarrow\uparrow} + \sum_x (P_{x\downarrow} - P_{x\uparrow}) \right] \cos \theta
\end{aligned} \tag{5}$$

We also introduce the probability L_a that atom a lays outside the qubit basis $\{|\uparrow\rangle, |\downarrow\rangle\}$, given by $L_a = \sum_x (P_{x\uparrow} + P_{x\downarrow}) + \sum_{x,x'} P_{x,x'}$ and similarly for atom b , $L_b = \sum_x (P_{\uparrow x} + P_{\downarrow x}) + \sum_{x,x'} P_{x,x'}$. From expression (4) and (5) the probabilities L_a and L_b are related to the mean value of $P_{a/b}(\theta)$ by the expression

$$\langle P_{a/b}(\theta) \rangle = \frac{1}{2} (1 - L_{a/b}) . \tag{6}$$

This expression is intuitive: the mean value of the probability for an atom to be recaptured, i.e. the atom is in state $|\downarrow\rangle$, is $1/2$ when there is no additional loss during the entangling sequence. When we take into account the probability to lose the atom, we simply multiply the probability in the absence of additional loss, $1/2$, with the probability to stay in the qubit basis $1 - L_{a/b}$.

The calculation gives the joint probability to recapture both atoms at the end of the

Raman rotation:

$$\begin{aligned}
P_{11}(\theta) &= P_{\downarrow\downarrow}(\theta) \\
&= \frac{1}{8} [P_{\uparrow\downarrow} + P_{\downarrow\uparrow} + 2\Re(\rho_{\downarrow\uparrow,\uparrow\downarrow}) + 3(P_{\uparrow\uparrow} + P_{\downarrow\downarrow})] \\
&\quad + \frac{1}{2}(P_{\downarrow\downarrow} - P_{\uparrow\uparrow}) \cos \theta \\
&\quad + \frac{1}{8} [P_{\downarrow\downarrow} + P_{\uparrow\uparrow} - P_{\uparrow\downarrow} - P_{\downarrow\uparrow} - 2\Re(\rho_{\downarrow\uparrow,\uparrow\downarrow})] \cos 2\theta .
\end{aligned} \tag{7}$$

Here, \Re denotes the real part. This expression exhibits terms oscillating at frequencies $\Omega_{\uparrow\downarrow}$ and $2\Omega_{\uparrow\downarrow}$. The term at $\Omega_{\uparrow\downarrow}$ reflects the imbalance between the states $|\uparrow, \uparrow\rangle$ and $|\downarrow, \downarrow\rangle$. We note also that this expression of P_{11} does not involve any loss terms, as it characterizes situations where both atoms are present at the end of the sequence. That is why we focus on this quantity for extracting the amount of entanglement between the two atoms.

Finally, we calculate the signal $\Pi(\theta)$, which is equal to the parity [20] when there are no losses from the qubit basis. We find the expression:

$$\begin{aligned}
\Pi(\theta) &= \frac{1}{2} \left[P_{\downarrow\downarrow} + P_{\uparrow\uparrow} - P_{\uparrow\downarrow} - P_{\downarrow\uparrow} + 2\Re(\rho_{\downarrow\uparrow,\uparrow\downarrow}) + 2 \sum_{x,x'} P_{xx'} \right] \\
&\quad + \sum_x (P_{x\uparrow} + P_{\uparrow x} - P_{x\downarrow} - P_{\downarrow x}) \cos \theta \\
&\quad + \frac{1}{2} [P_{\downarrow\downarrow} + P_{\uparrow\uparrow} - P_{\uparrow\downarrow} - P_{\downarrow\uparrow} - 2\Re(\rho_{\downarrow\uparrow,\uparrow\downarrow})] \cos 2\theta
\end{aligned} \tag{8}$$

This formula also presents oscillations at two frequencies, the one at $\Omega_{\uparrow\downarrow}$ being related this time to events where only one of the two atoms are present.

As a final remark on this model we point out that a global rotation with no control over the phase φ would not be suitable to analyze the Bell states $|\Psi^-\rangle = (|\uparrow, \downarrow\rangle - |\downarrow, \uparrow\rangle)/\sqrt{2}$ and $|\Phi^\pm\rangle = (|\uparrow, \uparrow\rangle \pm |\downarrow, \downarrow\rangle)/\sqrt{2}$. As an example, the antisymmetric state $|\Psi^-\rangle$ does not change under the rotation [20], whatever the phase φ . For the states $|\Phi^\pm\rangle$, the coherence $\rho_{\downarrow\downarrow,\uparrow\uparrow}$ acquires under the rotation a phase factor $e^{-i2\varphi}$. On a single realization of the experiment, the phase φ is fixed but the average over many realizations cancels out. The robustness of $|\Psi^+\rangle$ under fluctuations of φ is reminiscent of the fact that this state lies in a decoherence free subspace [21].

In the remaining part of the paper, we will use this model to extract from a single set of data the probability to lose one and two atoms, as well as the amount of entanglement.

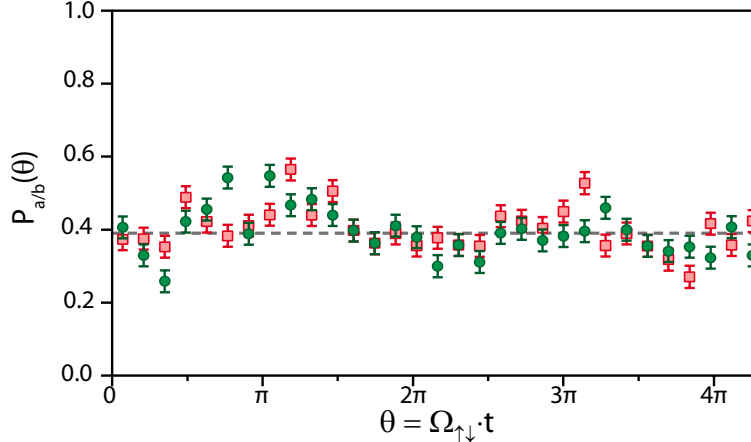


FIG. 3: Measured probabilities $P_a(\theta)$ (red squares) and $P_b(\theta)$ (green dots) to recapture each atom at the end of the entanglement procedure, followed by a Raman pulse on both atoms for different pulse durations. The dotted indicates the mean value of $P_{a/b}(\theta)$.

ANALYSIS OF THE LOSSES

Figure 3 shows the recapture probabilities $P_{a/b}(\theta)$ for each atom for different values of the Raman rotation angle. From equation (6) and the mean value of $P_{a/b}(\theta)$ deduced from the data we find $L_a = L_b = 0.22(1)$, confirming that the loss probability is the same for both atoms. Assuming independent losses for atoms a and b we find the probability to lose at least one of the two atoms $L_{\text{total}} = L_a(1 - L_b) + L_b(1 - L_a) + L_a L_b = 0.39(2)$. The recapture probability of a pair of atoms in the qubit basis $\{|\uparrow\rangle, |\downarrow\rangle\}$ is then $L_{\text{total}} = 1 - \text{tr}\hat{\rho}$, restricting the trace to pairs of atoms still present at the end of the entangling sequence in the states $|\uparrow\rangle$ and $|\downarrow\rangle$.

The loss channels can be separated in three classes. In the first category, independent of the Rydberg excitation and Raman rotation, we measured losses during the time the trap is switched off ($\sim 3\%$) as well as errors in the detection of the presence of the atom ($\sim 3\%$). For this first category, the loss channels $\{|x\rangle\}$ correspond to an atom in any internal state but which is lost from the tweezers.

In the second category, the losses are also physical and occur during the entangling and mapping pulses. These losses correspond to situations where one or two atoms have left the dipole traps, and are therefore absent when the Raman rotation and the measurement

take place. These losses are independent of the state detection and are mostly related to the fact that an atom left in the Rydberg state is lost, since it is not trapped in the dipole trap. Using a model based on Bloch equations including the 5 relevant states ($|\uparrow\rangle$, $|\downarrow\rangle$, $|5s_{1/2}, F=2, M=1\rangle$, $|5p_{1/2}, F=2, M=2\rangle$ and $|r\rangle$), we identify the following scenarios. Firstly, spontaneous emission from the $5p_{1/2}$ state populates the state $|\downarrow\rangle$ from which $\sim 7\%$ of the atoms get excited to the Rydberg state by the mapping pulse. Secondly, intensity fluctuations (5 %) and frequency fluctuations (3 MHz) of the excitation lasers reduce the efficiency of the mapping pulse so that $\sim 7\%$ of the atoms will not be transferred back from the Rydberg state to $|\downarrow\rangle$. For this second class, the loss channel $|x\rangle$ is any Rydberg states $|r\rangle$ which can be coupled by the two-photon transition including the one resulting, e.g. from an imperfect polarization of the lasers.

The third class of losses corresponds to atoms that are still present at the end of the entangling and mapping sequence, but which are in states different from $|\uparrow\rangle$ and $|\downarrow\rangle$, that is outside the qubit basis when the state measurement is performed. Because of the selection rules, the main possibility in our case is the spontaneous emission from the $5p_{1/2}$ to state $|x\rangle = |5s_{1/2}, F=2, M=1\rangle$ during the entangling and mapping pulses which is calculated to be only $\sim 2\%$, due to a small branching ratio. This third contribution is therefore small in our case. By adding the contributions of the three categories of losses we find a loss probability for each atom of 0.22, in agreement with the measured values of $L_{a/b}$.

Finally, we compare the probability $1 - L_{\text{total}} = 0.61(2)$ for a pair of atoms to be in states $|\uparrow\rangle$ or $|\downarrow\rangle$ with the probability $p_{\text{recap}} = 0.62(3)$ to recapture both atoms, irrespective of their internal states. Both values are almost identical, confirming that the dominant mechanism is a physical loss of the atoms before the state measurement.

PARTIAL STATE RECONSTRUCTION AND FIDELITY

In order to analyse the two-atom state we focus on the the joint recapture probability for atom pairs $P_{11}(\theta)$ shown in figure 4, since it incorporates no loss terms, as shown in equation (7). For the maximally entangled state $|\Psi^+\rangle$, $P_{11}(\theta)$ should oscillate between 0 and $1/2$ at a frequency $2\Omega_{\uparrow\downarrow}$, while here the data show oscillations at two frequencies $\Omega_{\uparrow\downarrow}$ and $2\Omega_{\uparrow\downarrow}$, with a reduced amplitude. From the measurement of $P_{11}(\theta)$ and the expression (7), we extract $P_{\downarrow\downarrow} = P_{11}(0)$ and $P_{\uparrow\uparrow} = P_{11}(\pi)$. Combining the value of the total losses L_{total} and

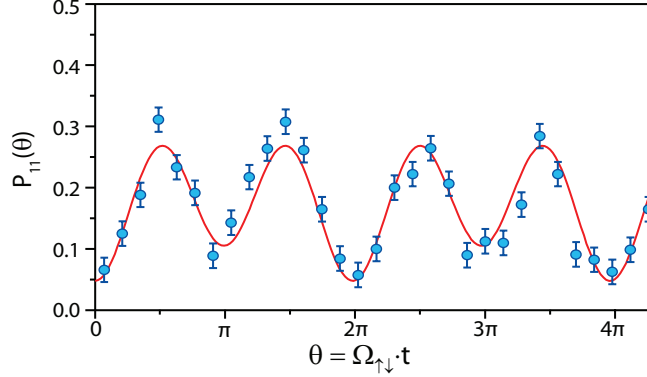


FIG. 4: Measured probability $P_{11}(\theta)$ to recapture the two atoms at the end of the entanglement procedure, followed by a Raman pulse on both atoms for different pulse durations. The data are fitted by a function of the form $y_0 + A \cos \Omega_{\uparrow\downarrow} t + B \cos 2\Omega_{\uparrow\downarrow} t$, according to the discussion in the text. The error bars on the data are statistical. The fit gives $y_0 = 0.17(2)$, $A = -0.03(1)$ and $B = -0.096$.

Matrix elements	Experimental values
$\rho_{\downarrow\downarrow,\downarrow\downarrow} = P_{\downarrow\downarrow}$	0.06 ± 0.02
$\rho_{\uparrow\uparrow,\uparrow\uparrow} = P_{\uparrow\uparrow}$	0.09 ± 0.02
$\rho_{\downarrow\uparrow,\downarrow\uparrow} + \rho_{\uparrow\downarrow,\uparrow\downarrow} = P_{\downarrow\uparrow} + P_{\uparrow\downarrow}$	0.46 ± 0.03
$\Re(\rho_{\downarrow\uparrow,\uparrow\downarrow})$	0.23 ± 0.04

TABLE I: Measured values of the density matrix elements characterizing the state prepared in the experiment extracted from $P_{11}(\theta)$. The error bars are statistical. Note that the restriction to the states $|\uparrow\rangle$ and $|\downarrow\rangle$ leads to $\text{tr}(\hat{\rho}) = 0.61$ because of the loss $L_{\text{total}} = 0.39(2)$ from the qubit basis.

the normalization condition $P_{\uparrow\downarrow} + P_{\downarrow\uparrow} + P_{\uparrow\uparrow} + P_{\downarrow\downarrow} + L_{\text{total}} = 1$, we get $P_{\uparrow\downarrow} + P_{\downarrow\uparrow}$. The mean value $\langle P_{11}(\theta) \rangle = [P_{\downarrow\uparrow} + P_{\uparrow\downarrow} + 3P_{\downarrow\downarrow} + 3P_{\uparrow\uparrow} + 2\Re(\rho_{\downarrow\uparrow,\uparrow\downarrow})]/8$ yields $\Re(\rho_{\downarrow\uparrow,\uparrow\downarrow})$. Table I summarizes the complete information about the density matrix $\hat{\rho}$ one can extract from global Raman rotations without control of φ .

As a cross-check of our data analysis, we look at the signal $\Pi(\theta)$ which is shown in figure 5. For the maximally entangled state $|\Psi^+\rangle$, the parity should oscillate between -1 and $+1$ with a frequency of $2\Omega_{\uparrow\downarrow}$, while here the observed $\Pi(\theta)$ oscillates at two frequencies, $\Omega_{\uparrow\downarrow}$ and $2\Omega_{\uparrow\downarrow}$ with reduced amplitude. From equation (8) we calculate $\Pi(\pi/2) = 2\Re(\rho_{\downarrow\uparrow,\uparrow\downarrow}) + \sum_{x,x'} P_{xx'}$.

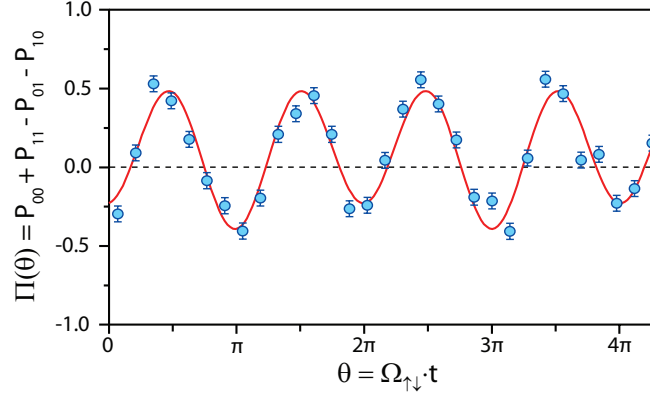


FIG. 5: Measured signal $\Pi(\theta)$ for different durations of the analysing Raman pulse. The data are fitted by a function of the form $y_0 + A \cos \Omega_{\uparrow\downarrow}t + B \cos 2\Omega_{\uparrow\downarrow}t$ as discussed in the text. The error bars on the data are statistical. The fit gives $y_0 = 0.08(1)$, $A = -0.07(1)$ and $B = -0.39(1)$.

Under the assumption that losses are independent for atoms a and b , as mentioned in section , $L_{\text{total}} = L_a + L_b - L_a L_b$. Combining this formula with the expressions of L_{total} , L_a and L_b given in section , we get $\sum_{x,x'} P_{xx'} = L_a L_b$. We then deduce the coherence $\Re(\rho_{\downarrow\uparrow,\uparrow\downarrow}) = 0.22(4)$, which is in good agreement with the value deduced from the analysis of $P_{11}(\theta)$ described above.

Our analysis allows us to calculate the fidelity of the entangling operation. This fidelity F is defined by $F = \langle \Psi^+ | \hat{\rho} | \Psi^+ \rangle = (P_{\downarrow\uparrow} + P_{\uparrow\downarrow})/2 + \Re(\rho_{\downarrow\uparrow,\uparrow\downarrow})$ with respect to the expected $|\Psi^+\rangle$ Bell state [22]. From the values in table I, we get $F = 0.46(4)$. This fidelity F is defined with respect to the initial number of atom pairs and includes events for which one or two atoms have been lost physically during the entangling sequence. That means F characterizes the whole entangling operation which is mainly limited by atom losses. As $F < 0.5$, this value does not prove entanglement between the atoms.

The quantum nature of the correlations between the two atoms is revealed if we calculate the fidelity $F_{\text{pairs}} = F/p_{\text{recap}}$ which characterizes the pairs of atoms effectively present at the end of the entangling sequence before state detection. From $p_{\text{recap}} = 0.62(3)$, we calculate $F_{\text{pairs}} = 0.74(7)$. This approach to take into account atom losses, is very similar to the one used in Bell inequality tests with photons based on *one-way polarizers* [23, 24]. In these experiments, the absence of a photon detection after the polarizer can be due to a photon with orthogonal polarization, or a photon that has been lost before reaching the polarizer.

Therefore, the total number of detected photon pairs is first measured by removing the polarizers, then the measurement of the polarization correlation is performed and the results are renormalized by the total number of photon pairs.

Our analysis gives also access to the fidelity $F_{\uparrow\downarrow} = F/\text{tr}\hat{\rho}$ which characterizes the entanglement of atom pairs which are still in the qubit basis $\{|\uparrow\rangle, |\downarrow\rangle\}$. We find $F_{\uparrow\downarrow} = 0.75(7)$, which is very close to F_{pairs} since the main mechanism for atom losses is the physical loss of one or two atoms from their traps. The fact that $F_{\text{pairs}} > 0.5$ and $F_{\uparrow\downarrow} > 0.5$ proves that the two atoms are entangled. We can identify two effects lowering the fidelity with respect to the ideal case. Firstly, an imperfect Rydberg blockade leads to the excitation of both atoms (probability $\sim 10\%$ [16]) and their subsequent mapping to the state $|\downarrow, \downarrow\rangle$, resulting in a non-zero component of $P_{\downarrow\downarrow}$. Secondly, the excess value of $P_{\uparrow\uparrow}$ is explained by spontaneous emission from the state $5p_{1/2}$ as well as imperfect Rydberg excitation from the two atom state $|\uparrow, \uparrow\rangle$. We note that in the present status of the experiment, the influence of the residual motion of the atoms in their traps is negligible on the fidelity (for more details, see [14]).

CONCLUSION

In conclusion, we have used global Raman rotations to analyze the entanglement of two atoms which is created using the Rydberg blockade. Our analysis is based on a model taking into account losses of atoms. We have found that the 62% pairs of atoms remaining at the end of the sequence are in a state with a fidelity 0.74(7) with respect to the expected $|\Psi^+\rangle$, showing the non-classical origin of the correlations. Future work will be devoted to the measurement of the coherence time of the entangled state, as well as to the improvement of the fidelity and the state detection scheme.

We thank M. Barbieri, M. Müller, R. Blatt, D. Kielpinski and P. Maunz for discussions. We acknowledge support from the European Union through the Integrated Project SCALA, IARPA and the Institut Francilien de Recherche sur les Atomes Froids (IFRAF). A. Gaëtan and C. Evellin are supported by a DGA fellowship. T. Wilk is supported by IFRAF.

[1] R. Blatt, and D. Wineland, Nature **453**, 1008 (2008).

- [2] E. Hagley, X. Maître, G. Nogues, C. Wunderlich, M. Brune, J. M. Raimond, and S. Haroche, *Phys. Rev. Lett.* **79**, 1 (1997).
- [3] O. Mandel, M. Greiner, A. Widera, T. Rom, T. W. Hänsch, and I. Bloch, *Nature* **425**, 937 (2003).
- [4] M. Anderlini, P. J. Lee, B. L. Brown, J. Sebby-Strabley, W. D. Phillips, and J. V. Porto, *Nature* **448**, 452 (2007).
- [5] W. S. Bakr, J. I. Gillen, A. Peng, S. Fölling, and M. Greiner, *Nature* **462**, 74 (2009).
- [6] S. Bergamini, B. Darquié, M. Jones, L. Jacubowicz, A. Browaeys, and P. Grangier, *J. Opt. Soc. Am. B* **21**, 1889 (2004).
- [7] K. D. Nelson, X. Li, and D. S. Weiss, *Nature Physics* **3**, 556 (2007).
- [8] D. Jaksch, J. I. Cirac, P. Zoller, S. L. Rolston, R. Côté, and M. D. Lukin, *Phys. Rev. Lett.* **85**, 2208 (2000).
- [9] M. D. Lukin, M. Fleischhauer, R. Côté, L. M. Duan, D. Jaksch, J. I. Cirac, and P. Zoller, *Phys. Rev. Lett.* **87**, 037901 (2001).
- [10] M. Saffman, and T. G. Walker, *Phys. Rev. A* **72**, 022347 (2005).
- [11] D. Møller, L. B. Madsen, and K. Mølmer, *Phys. Rev. Lett.* **100**, 170504 (2008).
- [12] M. Müller, I. Lesanovsky, H. Weimer, H. P. Büchler, and P. Zoller, *Phys. Rev. Lett.* **102**, 170502 (2009).
- [13] L. Isenhower, E. Urban, X. L. Zhang, A. T. Gill, T. Henage, T. A. Johnson, T. G. Walker, and M. Saffman, arXiv:0907.5552 (2009).
- [14] T. Wilk, A. Gaëtan, C. Evellin, J. Wolters, Y. Miroshnychenko, P. Grangier, and A. Browaeys, arXiv:0908.0454 (2009).
- [15] E. Urban, T. A. Johnson, T. Henage, L. Isenhower, D. D. Yavuz, T. G. Walker, and M. Saffman, *Nature Phys.* **5**, 110 (2009).
- [16] A. Gaëtan, Y. Miroshnychenko, T. Wilk, A. Chotia, M. Viteau, D. Comparat, P. Pillet, A. Browaeys, and P. Grangier, *Nature Phys.* **5**, 115 (2009).
- [17] N. Schlosser, G. Reymond, I. Protsenko, and P. Grangier, *Nature* **411**, 1024 (2001).
- [18] T. G. Walker, and M. Saffman, *Phys. Rev. A* **77**, 032723 (2008).
- [19] M. P. A. Jones, J. Beugnon, A. Gaëtan, J. Zhang, G. Messin, A. Browaeys, and P. Grangier, *Phys. Rev. A* **75**, 040301 (2007).
- [20] Q. A. Turchette, C. S. Wood, B. E. King, C. J. Myatt, D. Leibfried, W. M. Itano, C. Monroe,

- and D. J. Wineland, Phys. Rev. Lett. **81**, 3631 (1998).
- [21] H. Häffner, F. Schmidt-Kaler, W. Hänsel, C.F. Roos, T. Körber, M. Chwalla, M. Riebe, J. Benhelm, U.D. Rapol, C. Becher, and R. Blatt, App. Phys. B **81**, 151 (2005).
- [22] C. A. Sackett, D. Kielpinski, B. E. King, C. Langer, V. Meyer, C. J. Myatt, M. Rowe, Q. A. Turchette, W.M. Itano, D. J. Wineland, and C. Monroe, Nature **404**, 256 (2000).
- [23] S. J. Freedman, and J.F. Clauser, Phys. Rev. Lett. **28**, 938 (1972).
- [24] A. Aspect, P. Grangier, and G. Roger, Phys. Rev. Lett. **47**, 460 (1981).
- [25] For a discussion of the case where atoms move, see reference [14].
- [26] This reduction of the dipole trap depth decreases the temperature of the atoms and we have found that it also leads to a better optical pumping.
- [27] This statement assumes that there is no other Zeeman state of the $(5s_{1/2}, F = 1)$ manifold populated than $|\downarrow\rangle = |5s_{1/2}, F = 1, M = 1\rangle$. This is indeed the case in our experiment, as explained in section .